6178 *Inorg. Chem.* **2009**, *48*, 6178–6191
DOI: 10.1021/ic9005136

Inorganic Chemistry
Article

Benzothiazole- and Benzoxazole-Substituted Pyridine-2-Carboxylates as Efficient Sensitizers of Europium Luminescence

Nail M. Shavaleev, Rosario Scopelliti, Frédéric Gumy, and Jean-Claude G. Bünzli*

École Polytechnique Fédérale de Lausanne, Laboratory of Lanthanide Supramolecular Chemistry, BCH 1405, CH-1015 Lausanne, Switzerland

Received March 16, 2009

A facile synthesis of benzothiazole- and benzoxazole-substituted pyridine-2-carboxylic acids has been developed. These ligands form mononuclear nine-coordinate complexes [Ln(κ^3-ligand)$_2$(κ^1-ligand)(H$_2$O)$_2$] with light and heavy trivalent lanthanides, as established from the X-ray analysis of 11 complexes. A crystal structure of a minor product, the anhydrous nine-coordinate complex [Eu(κ^3-L)$_3$], has also been determined. Photophysical studies of gadolinium chelates indicate that the triplet states of the new ligands are located at 20400−21400 cm^{-1}. The ligands are good sensitizers of the europium luminescence with ligand-to-metal energy transfer efficiency in the range 60−100%. The overall quantum yields of the europium emission are substantial, 12−14% in the solid state, and increase to 29−39% upon replacement of two metal-coordinated water molecules with dimethylsulfoxide in solution. The luminescence of near-infrared emitting lanthanides is also sensitized, but quantum yields are much smaller, reaching 0.17% for neodymium and 1.25% for ytterbium in DMSO, while energy transfer efficiencies for these two ions are below 50%.

Introduction

Trivalent lanthanide (Ln^{III}) complexes are exceedingly useful luminescent tags for bioanalytical applications[1] and serve as light-emitting materials in optical devices.[2] Their line-like emission spectra span visible[3] and near-infrared range,[4] and long excited state lifetimes allow easy time-resolved detection.[1b] On the other hand, the Laporte-forbidden f-f transitions have weak dipole strengths, and the excited states may be easily quenched by high-energy vibrations, particularly O−H oscillators from water molecules both in the inner and outer coordination spheres.[5] To achieve bright emission, a lanthanide ion needs a carefully tailored environment consisting of ligands with adequate chromophoric groups to harvest light and subsequently populate the metal-ion excited states through energy transfer,[6] while simultaneously providing a rigid and protective coordination shell to minimize non-radiative deactivation. Taking into account the thermodynamics of complex formation and the large coordination numbers (commonly 8−10) required for Ln^{III} ions, it is therefore not surprising that anionic polydentate donors are preferred ligands for lanthanides. In particular, monoanionic tridentate receptors are especially interesting because they saturate the coordination sphere of the Ln^{III} ions upon formation of tris complexes and fully compensate their charge, an advantage when it comes to their application as in vivo probes, or in optical devices.

Carboxylates are hard Lewis bases and are known to bind strongly to Ln^{III} ions which have a pronounced hard Lewis acid character. When modified with a light-harvesting group, they are adequate luminescence sensitizers.[7] Picolinate (pyridine-2-carboxylate) is a bidentate N,O-donor ligand, which finds use in the design of coordination networks,[8] and emitting materials[9] based on lanthanide ions. Its grafting

*To whom correspondence should be addressed. E-mail: jean-claude.bunzli@eplf.ch.

(1) (a) Hovinen, J.; Guy, P. M. *Bioconjugate Chem.* **2009**, *20*, 404. (b) Bünzli, J.-C. G. *Chem. Lett.* **2009**, *38*, 104. (c) Gunnlaugsson, T.; Stomeo, F. *Org. Biomol. Chem.* **2007**, *5*, 1999.

(2) (a) de Bettencourt-Dias, A. *Dalton Trans.* **2007**, 2229. (b) Katkova, M. A.; Vitukhnovsky, A. G.; Bochkarev, M. N. *Russ. Chem. Rev.* **2005**, *74*, 1089. (c) Kido *J. Chem. Rev.* **2002**, *102*, 2357.

(3) Bünzli, J.-C. G.; Piguet, C. *Chem. Soc. Rev.* **2005**, *34*, 1048.

(4) Comby, S.; Bünzli, J.-C. G. Lanthanide near-infrared luminescence in molecular probes and devices. In *Handbook on the Physics and Chemistry of Rare Earths*; Gschneidner, J. A., Jr., Bünzli, J.-C. G., Pecharsky, V., Eds.; Elsevier Science B.V.: Amsterdam, 2007; Vol. *37*, Chapter 235, pp 217−470, and references therein.

(5) Beeby, A.; Clarkson, I. M.; Dickins, R. S.; Faulkner, S.; Parker, D.; Royle, L.; de Sousa, A. S.; Williams, J. A. G.; Woods, M. *J. Chem. Soc., Perkin Trans. 2* **1999**, 493.

(6) de Sá, G. F.; Malta, O. L.; de Mello Donegá, C.; Simas, A. M.; Longo, R. L.; Santa-Cruz, P. A.; da Silva, E. F., Jr. *Coord. Chem. Rev.* **2000**, *196*, 165.

(7) (a) Viswanathan, S.; de Bettencourt-Dias, A. *Inorg. Chem.* **2006**, *45*, 10138. (b) Shyni, R.; Biju, S.; Reddy, M. L. P.; Cowley, A. H.; Findlater, M. *Inorg. Chem.* **2007**, *46*, 11025. (c) Harbuzaru, B. V.; Corma, A.; Rey, F.; Atienzar, P.; Jordá, J. L.; García, H.; Ananias, D.; Carlos, L. D.; Rocha, J. *Angew. Chem., Int. Ed.* **2008**, *47*, 1080.

(8) Li, W.; Wang, X.-L.; Song, X.-Y.; Li, L.-C.; Liao, D.-Z.; Jiang, Z.-H. *J. Mol. Struct.* **2008**, *885*, 1.

(9) (a) Soares-Santos, P. C. R.; Nogueira, H. I. S.; Félix, V.; Drew, M. G. B.; Sá Ferreira, R. A.; Carlos, L. D.; Trindade, T. *Inorg. Chem. Commun.* **2003**, *6*, 1234. (b) Hong, J. H.; Oh, Y.; Kim, Y.; Kang, S. K.; Choi, J.; Kim, W. S.; Lee, J. I.; Kim, S.-J.; Hur, N. H. *Cryst. Growth Des.* **2008**, *8*, 1364.

Published on Web 05/14/2009

with an additional coordinating function in position 6 results in tridentate chelating units featuring O,N,O or N,N,O donors. Typical extra functions are carboxylate,[10] amide,[11] alkylamine,[12] or heterocycles such as pyridine,[13,14] pyrazole,[15] or benzimidazole.[16,17] These ligands have generated a fruitful coordination chemistry for the lanthanides and can serve as building blocks to develop more elaborate polydentate ligands. For instance, our research team has recently demonstrated that lanthanide complexes with benzimidazole-substituted pyridine-2-carboxylic acids can be used in time-resolved luminescence imaging of live cells.[17]

Other potential modifier group for picolinate is benzoxazole; indeed this unit is known to sensitize lanthanide luminescence,[18] and it is a component of a naturally occurring ionophore calcimycin.[19] Until now, benzoxazoles and their sulfur-substituted counterparts, benzothiazoles, have been rarely used in lanthanide coordination chemistry.[20−24] We have recently attached benzoxazole substituents on a 8-hydroxyquinolinate framework and explored their versatility for controlling lanthanide luminescence in the near-infrared.[24] In this paper, we present the synthesis of substituted pyridine-2-carboxylic acids that combine a tridentate monoanionic N,N,O binding site and a light-harvesting benzoxazole or benzothiazole chromophore (Scheme 1). We anticipated that a combination of these functions would provide ligands and complexes with useful optical properties. A simple and straightforward synthesis of these ligands has therefore been developed, and we report the isolation, crystal structures, and photophysical properties of their lanthanide complexes (Chart 1).

Scheme 1. Synthesis of Benzothiazole- and Benzoxazole-Substituted Pyridine-2-Carboxylic Acids[a]

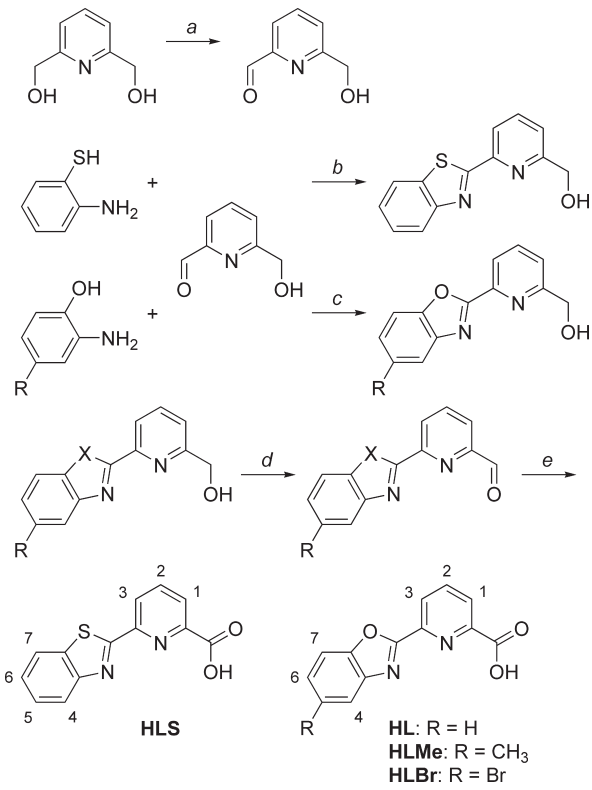

[a] Reaction conditions: (a) SeO_2, dioxane, under N_2, 65°C; (b) DMSO, under N_2, 140°C; (c) (i) dioxane/ethanol, under N_2, 110°C; (ii) DDQ, CH_2Cl_2, under N_2, sonication, room temp.−40°C; (d) SeO_2, dioxane, under N_2, 110°C; (e) H_2O_2, formic acid, under air, 0°C.

Results and Discussion

Synthesis. Of the ligands reported herein, only HL has been described previously; it has been prepared in small scale from 2-phenylbenzoxazole via bioconversion with *Escherichia coli* cells carrying an adequate gene.[25] To make these ligands accessible in large quantities, we have devised a simple and convenient synthesis starting from 2-pyridinecarboxaldehyde-6-methanol (Scheme 1). Although this compound is known,[26] we have modified its synthesis and obtained it in 80% yield by mono-oxidation of 2,6-pyridinedimethanol with SeO_2 at 65 °C in dioxane. Selenium dioxide is commonly used to oxidize 2,6-pyridinedimethanol to 2,6-pyridinedicarboxaldehyde.[27] However, we have noted that this oxidation occurs stepwise and with a strong dependence on temperature; as a consequence, it can be driven to yield selectively the mono-oxidized product by a judicious selection of both the temperature and the ratio of

(10) (a) Gassner, A.-L.; Duhot, C.; Bünzli, J.-C. G.; Chauvin, A.-S. *Inorg. Chem.* **2008**, *47*, 7802. (b) D'Aléo, A.; Picot, A.; Beeby, A.; Williams, J. A. G.; Le Guennic, B.; Andraud, C.; Maury, O. *Inorg. Chem.* **2008**, *47*, 10258. (c) Han, M.; Zhang, H.-Y.; Yang, L.-X.; Jiang, Q.; Liu, Y. *Org. Lett.* **2008**, *10*, 5557.

(11) (a) Lessmann, J. J.; Horrocks, W. DeW., Jr. *Inorg. Chem.* **2000**, *39*, 3114. (b) An, B.-L.; Gong, M.-L.; Zhang, J.-M.; Zheng, S.-L. *Polyhedron* **2003**, *22*, 2719. (c) Senegas, J. M.; Bernardinelli, G.; Imbert, D.; Bünzli, J. C. G.; Morgantini, P. Y.; Weber, J.; Piguet, C. *Inorg. Chem.* **2003**, *42*, 4680.

(12) (a) Chatterton, N.; Bretonniere, Y.; Pécaut, J.; Mazzanti, M. *Angew. Chem., Int. Ed.* **2005**, *44*, 7595. (b) Mato-Iglesias, M.; Roca-Sabio, A.; Pálinkás, Z.; Esteban-Gómez, D.; Platas-Iglesias, C.; Tóth, E.; de Blas, A.; Rodríguez-Blas, T. *Inorg. Chem.* **2008**, *47*, 7840.

(13) (a) Comby, S.; Imbert, D.; Chauvin, A.-S.; Bünzli, J.-C. G.; Charbonnière, L. J.; Ziessel, R. F. *Inorg. Chem.* **2004**, *43*, 7369. (b) Kottas, G. S.; Mehlstäubl, M.; Fröhlich, R.; De Cola, L. *Eur. J. Inorg. Chem.* **2007**, 3465.

(14) (a) Charbonnière, L. J.; Ziessel, R.; Guardigli, M.; Roda, A.; Sabbatini, N.; Cesario, M. *J. Am. Chem. Soc.* **2001**, *123*, 2436. (b) Ulrich, G.; Bedel, S.; Picard, C. *Tetrahedron Lett.* **2002**, *43*, 8835.

(15) (a) Charbonnière, L. J.; Ziessel, R. *Helv. Chim. Acta* **2003**, *86*, 3402. (b) Brunet, E.; Juanes, O.; Rodríguez-Blasco, M. A.; Vila-Nova, S. P.; Rodríguez-Ubis, J. C. *Tetrahedron Lett.* **2007**, *48*, 1353.

(16) André, N.; Jensen, T. B.; Scopelliti, R.; Imbert, D.; Elhabiri, M.; Hopfgartner, G.; Piguet, C.; Bünzli, J.-C. G. *Inorg. Chem.* **2004**, *43*, 515.

(17) (a) Chauvin, A.-S.; Comby, S.; Song, B.; Vandevyver, C. D. B.; Bünzli, J.-C. G. *Chem.Eur. J.* **2008**, *14*, 1726. (b) Deiters, E.; Song, B.; Chauvin, A.-S.; Vandevyver, C. D. B.; Gumy, F.; Bünzli, J.-C. G. *Chem.Eur. J.* **2009**, *15*, 885.

(18) Thakur, P.; Chakravortty, V.; Dash, K. C. *Ind. J. Chem. A* **1999**, *38*, 1223.

(19) (a) Albin, M; Cader, B. M.; Horrocks, W. DeW., Jr. *Inorg. Chem.* **1984**, *23*, 3045. (b) Divakar, S.; Easwaran, K. R. K. *Biophys. Chem.* **1987**, *27*, 139.

(20) Rackham, D. M. *Spectrosc. Lett.* **1980**, *13*, 517.

(21) Drew, M. G. B.; Hill, C.; Hudson, M. J.; Iveson, P. B.; Madic, C.; Vaillant, L.; Youngs, T. G. A. *New J. Chem.* **2004**, *28*, 462.

(22) Gao, L.-H.; Guan, M.; Wang, K.-Z.; Jin, L.-P.; Huang, C.-H. *Eur. J. Inorg. Chem.* **2006**, 3731.

(23) (a) Katkova, M. A.; Borisov, A. V.; Fukin, G. K.; Baranov, E. V.; Averyushkin, A. S.; Vitukhnovsky, A. G.; Bochkarev, M. N. *Inorg. Chim. Acta* **2006**, *359*, 4289. (b) Roger, M.; Arliguie, T.; Thuéry, P.; Ephritikhine, M. *Inorg. Chem.* **2008**, *47*, 3863.

(24) Shavaleev, N. M.; Scopelliti, R.; Gumy, F.; Bünzli, J.-C. G. *Inorg. Chem.* **2009**, *48*, 2908.

(25) Shindo, K.; Osawa, A.; Nakamura, R.; Kagiyama, Y.; Sakuda, S.; Shizuri, Y.; Furukawa, K.; Misawa, N. *J. Am. Chem. Soc.* **2004**, *126*, 15042.

(26) (a) Ziessel, R.; Nguyen, P.; Douce, L.; Cesario, M.; Estournes, C. *Org. Lett.* **2004**, *6*, 2865. (b) Artali, R.; Botta, M.; Cavallotti, C.; Giovenzana, G. B.; Palmisano, G.; Sisti, M. *Org. Biomol. Chem.* **2007**, *5*, 2441.

(27) (a) Alcock, N. W.; Kingston, R. G.; Moore, P.; Pierpoint, C. *J. Chem. Soc., Dalton Trans.* **1984**, 1937. (b) Luening, U.; Baumstark, R.; Peters, K.; Von Schnering, H. G. *Liebigs Ann. Chem.* **1990**, 129.

Chart 1. New Lanthanide Complexes

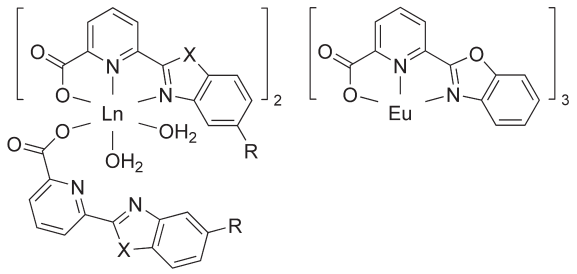

X = S; **R** = H
X = O; **R** = H, CH_3, Br
Ln = La, Nd, Eu, Gd, Tb, Yb

reagents. This simple method, which, surprisingly, has not been described before, is more convenient to use and easier to scale-up compared to the known mono-oxidation of 2,6-pyridinedimethanol with MnO_2.[26]

The benzothiazole ring was incorporated into ligand HLS by reaction of 2-pyridinecarboxaldehyde-6-methanol with 2-aminothiophenol in DMSO at 140 °C.[28] The benzoxazole ring[29] was prepared by a two-step, one-pot reaction of 2-pyridinecarboxaldehyde-6-methanol with 2-aminophenol. In the first step, a Schiff base was obtained in quantitative yield, which, in the second step, was oxidized to benzoxazole with 2,3-dichloro-5,6-dicyano-1,4-benzoquinone (DDQ).[29] The resulting fused heterocycle-substituted pyridine-2-methanols were oxidized with SeO_2 at 110 °C in dioxane to give pyridine-2-carboxaldehydes. The oxidation is selective, and SeO_2 does not oxidize the methyl group of the benzoxazole ring (see the synthesis of precursor LMe-CHO in the Supporting Information). Finally, pyridine-2-carboxaldehydes were oxidized by H_2O_2 in formic acid at 0 °C to yield pyridine-2-carboxylic acids.[30] Again, oxidation is selective and does not result in side reactions such as N-oxide formation or oxidative degradation. The ligands were obtained as white solids and were characterized by ^{1}H NMR spectroscopy and C, H, N-elemental analysis.

The ligands HLMe and HLBr containing a methyl group as a mild electron donor or a bromine as a mild electron acceptor and a "heavy atom", respectively, have been prepared with the purpose of probing the influence of electronic factors on the ligand-to-metal energy transfer. Furthermore, the presence of a bromine substituent in HLBr opens the way for subsequent modifications of these ligands by carbon−carbon or carbon−heteroatom coupling protocols.

Lanthanide complexes have been obtained as white solids from tetrahydrofuran (THF)/water solutions starting from stoichiometric 3:3:1 molar ratios of the ligand, base (NaOH), and $LnCl_3 \cdot nH_2O$. Although we expected that anhydrous complexes [Ln(κ^3-ligand)$_3$] would be formed in this reaction, the analytical data did not support this assumption: C, H, N-elemental analysis suggested the presence of crystallization water in the complexes, and crystallographic and photophysical studies allowed us to formulate them as bis-aqua species [Ln(κ^3-ligand)$_2$(κ^1-ligand)(H_2O)$_2$]·*solv* (*solv*: H_2O, THF) (Chart 1). The complexes are air and moisture stable. They are insoluble in water and common organic solvents, apart from coordinating ones, such as DMSO.

X-ray Structural Studies. Single crystals suitable for X-ray analysis could be obtained for 11 complexes [Ln(κ^3-ligand)$_2$(κ^1-ligand)(H_2O)$_2$]·*solv* (*solv*: CH_3CN, C_2H_5OH, or H_2O). The corresponding structures include at least one example for each of the four ligands (HLS, HL, HLMe, HLBr), and for each of the ions studied (Nd, Eu, Gd, Tb, Yb), apart from La. In addition, we have obtained single crystals of the anhydrous nine-coordinate complex [Eu(κ^3-L)$_3$] by recrystallization of a small batch (1−2 mg) of [Eu(κ^3-L)$_2$(κ^1-L)(H_2O)$_2$]·H_2O from ethanol. We believe this anhydrous complex to be either a minor product in the synthesis or formed during recrystallization from ethanol. An attempted recrystallization of a number of other complexes from ethanol, namely, [Ln(LS)$_3$(H_2O)$_2$]·nH_2O (Ln: Eu, Gd, Tb), [Tb(L)$_3$(H_2O)$_2$], and [Gd(LMe)$_3$(H_2O)$_2$], provided the expected bis-aqua species in every case, as established by the X-ray analysis. The resulting molecular structures are shown in Figure 1, and selected parameters are collected in Table 1.

The following common features are observed for the complexes [Ln(κ^3-ligand)$_2$(κ^1-ligand)(H_2O)$_2$]. (i) The lanthanide is nine-coordinated by one κ^1-bonded ligand connected via the carboxylate, two κ^3-bonded ligands, and two water molecules. The same coordination number is observed for the light and heavy lanthanides (Nd, Eu, Gd, Tb, Yb). (ii) The coordination environment around the lanthanide ions can be described as a distorted tricapped trigonal prism (Figure 2). The capping positions are occupied by two N atoms of pyridine rings from the κ^3-bonded ligands and a carboxylate O atom from the κ^1-bonded ligand (these atoms form a plane containing the lanthanide ion). Each of the triangular faces of the prism is defined by O(water), O(carboxylate), and N(fh) atoms; these faces are nearly parallel, the dihedral angle between them being 2.40−6.30°. (iii) The Ln-N and Ln-O bonds decrease while bite angles increase for heavier lanthanides, as a result of the lanthanide contraction; exceptions to these trends are sometimes observed in going from Eu to Gd, or Gd to Tb. (iv) The average Ln-N(fh) bond length for benzoxazole (L^-) is shorter by 0.028−0.071 Å compared to benzothiazole (LS^-). (v) The Ln-O (carboxylate) bond to the κ^1-ligand is shorter compared to the κ^3−ligand by 0.0078−0.021 Å for benzothiazole, and 0.02−0.068 Å for benzoxazole complexes. It may be explained by the rigidity of the ligands, coupled with the necessity to conform to the individual bite angles of the N,O pyridine-2-carboxylate and N,N pyridine-heterocycle binding sites, which may hinder a more optimized κ^3−binding. (vi) The imine nitrogen atoms of the pyridine and the fused heterocycle in the κ^1-ligand are located in trans position to each other, probably to minimize electrostatic interaction of their lone electron pairs. (vii) The two metal-coordinated water molecules form hydrogen bonds with a carbonyl oxygen of the ligand belonging to either the same or another complex molecule. The κ^1-bonded and κ^3-bonded ligands participate in only one type of H-bond, intramolecular for the former and intermolecular for the latter. One of the two

(28) Deligeorgiev, T. C. *Dyes Pigments* **1990**, *12*, 243.
(29) Giménez, R.; Oriol, L.; Piñol, M.; Serrano, J. L.; Viñuales, A. I.; Fisher, T.; Stumpe, J. *Helv. Chim. Acta* **2006**, *89*, 304.
(30) Dodd, R. H.; Le Hyaric, M. *Synthesis* **1993**, 295.

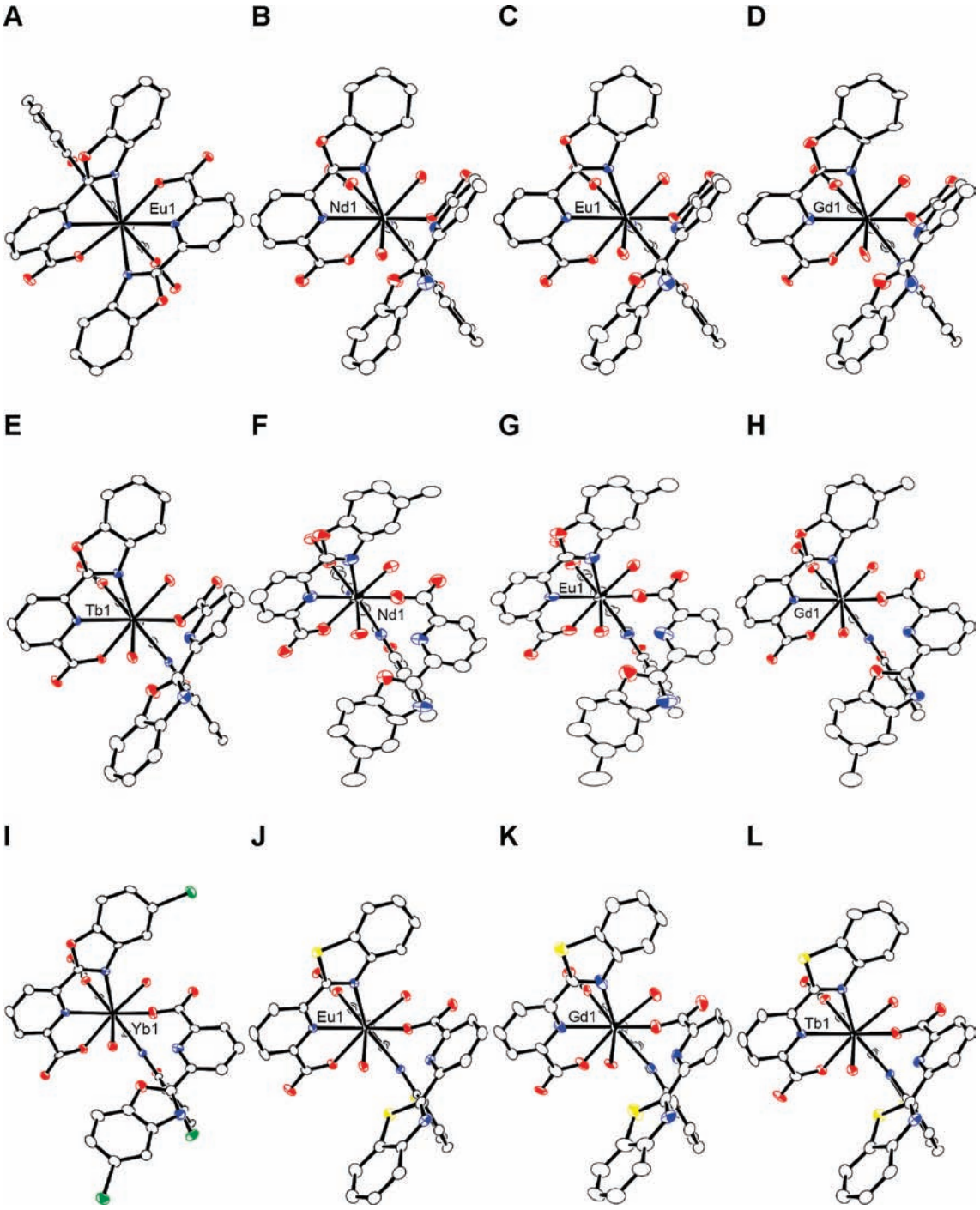

Figure 1. Molecular structures of the Ln^{III} complexes (50% probability ellipsoids, H atoms and co-crystallized solvent molecules omitted). Heteroatoms: O, red; N, blue; S, yellow; Br, green; Ln, black. **A**: $[Eu(L)_3]$. **B**-**E**: $[Ln(L)_3(H_2O)_2]$, Ln = Nd, Eu, Gd, Tb. **F**−**H**: $[Ln(LMe)_3(H_2O)_2]$, Ln = Nd, Eu, Gd. **I**: $[Yb(LBr)_3(H_2O)_2]$. **J**−**L**: $[Ln(LS)_3(H_2O)_2]$, Ln = Eu, Gd, Tb.

water molecules in the complex forms an intermolecular H-bond only (1.653−1.827 Å), while the other molecule forms two H-bonds, intermolecular (1.708−1.846 Å) and intramolecular (1.920−2.113 Å). The presence of intermolecular interactions results in the formation of a one-dimensional (1D)-chain polymeric structure which may explain the low solubility of the complexes in organic solvents. Each complex is bound to the next one within the 1D chain by two H-bonds.

In the anhydrous complex $[Eu(\kappa^3\text{-}L)_3]$, the europium ion is nine-coordinated by three ligands arranged in an "up-up-down" fashion. Its coordination environment can also be described as a distorted tricapped trigonal prism, with the N atoms of the pyridine rings occupying the capping positions and forming a plane which contains the Eu atom (Figure 2). The triangular faces of the prism are defined by [two O(carboxylate) and N(fh)] or [two N(fh) and O(carboxylate)] atoms; the dihedral angle between them is 13.51°, being larger than in the corresponding bis-hydrate complex, 5.54°.

Common structural features for all the analyzed complexes can be summarized as follows. (i) The Ln^{III} ion is

Table 1. Selected Structural Parameters for the Lanthanide Complexes[a]

complex	bond lengths (Å)[b]				angles (deg)				
	Ln−O	Ln−N(py)	Ln−N(fh)	Ln−OH_2	O−Ln−N(py)	N(py)−Ln−N(fh)	py−fh[e]	O···HOH (Å)[c]	Ln−Ln (Å)[d]
$[Nd(L)_3(H_2O)_2]$	2.413(6)	2.648(6)	2.738(6)	[1] 2.454(6)	62.96(19)	61.7(2)	8.91	[1] 1.705	8.148
	2.425(6)	2.648(7)	2.675(7)	[2] 2.475(6)	62.6(2)	61.9(2)	5.43	[2] 1.708	
	2.393(6)						14.00	[2] *2.010*	
	2.410	**2.648**	**2.707**	**2.465**	**62.8**	**61.8**			
$[Eu(L)_3(H_2O)_2]$	2.383(3)	2.603(4)	2.630(4)	[1] 2.407(3)	63.58(11)	62.38(12)	8.23	[1] 1.710	8.122
	2.387(4)	2.598(4)	2.698(4)	[2] 2.422(3)	63.29(12)	62.76(12)	5.72	[2] 1.708	
	2.352(4						13.28	[2] *1.937*	
	2.374	**2.601**	**2.664**	**2.415**	**63.4**	**62.6**			
$[Eu(L)_3]$	2.3644(14)	2.5530(16)	2.6410(16)		64.55(5)	63.69(5)	3.80		8.617
	2.3669(14)	2.5934(16)	2.7614(16)		63.98(5)	61.66(5)	12.13		
	2.3733(13)	2.5293(17)	2.6888(16)		65.19(5)	63.73(5)	8.57		
	2.368	**2.559**	**2.697**		**64.6**	**63.0**	**8.17**		
$[Gd(L)_3(H_2O)_2]$	2.363(7)	2.580(8)	2.701(8)	[1] 2.396(6)	63.0(2)	63.0(2)	7.89	[1] 1.770	8.102
	2.370(7)	2.568(8)	2.607(8)	[2] 2.404(7)	63.9(2)	63.1(3)	5.61	[2] 1.846	
	2.322(7)						12.53	[2] *1.920*	
	2.352	**2.574**	**2.654**	**2.400**	**63.5**	**63.1**			
$[Tb(L)_3(H_2O)_2]$	2.3505(16)	2.5792(19)	2.666(2)	[1] 2.4026(16)	64.18(6)	62.80(6)	9.22	[1] 1.707	8.108
	2.3821(16)	2.5886(19)	2.604(2)	[2] 2.4036(16)	63.50(6)	62.97(6)	5.94	[2] 1.722	
	2.3151(17)						11.61	[2] *1.940*	
	2.349	**2.584**	**2.635**	**2.403**	**63.8**	**62.9**			
$[Nd(LMe)_3(H_2O)_2]$	2.436(11)	2.636(12)	2.690(12)	[1] 2.472(10)	62.1(3)	62.9(4)	8.37	[1] 1.800	8.265
	2.445(10)	2.645(11)	2.725(11)	[2] 2.489(11)	62.6(3)	62.3(3)	3.86	[2] 1.796	
	2.401(11)						7.50	[2] *1.957*	
	2.427	**2.641**	**2.708**	**2.481**	**62.4**	**62.6**			
$[Eu(LMe)_3(H_2O)_2]$	2.398(9)	2.594(11)	2.680(10)	[1] 2.430(10)	63.8(3)	62.6(3)	3.37	[1] 1.728	8.228
	2.402(10)	2.585(12)	2.658(11)	[2] 2.443(10)	62.7(3)	63.7(4)	9.12	[2] 1.826	
	2.338(11)						8.71	[2] *1.997*	
	2.379	**2.590**	**2.669**	**2.437**	**63.3**	**63.2**			
$[Gd(LMe)_3(H_2O)_2]$	2.384(4)	2.557(5)	2.617(4)	[1] 2.425(4)	63.68(13)	63.46(14)	10.62	[1] 1.828	8.213
	2.391(4)	2.578(5)	2.644(5)	[2] 2.435(4)	63.63(13)	63.18(14)	2.52	[1] *1.972*	
	2.391(4)						7.63	[2] 1.827	
	2.391(4)	**2.568**	**2.631**	**2.430**	**63.7**	**63.3**			
$[Yb(LBr)_3(H_2O)_2]$	2.318(4)	2.520(5)	2.617(5)	[1] 2.342(4)	65.30(15)	63.94(16)	3.63	[1] 1.793	8.124
	2.323(4)	2.500(5)	2.623(5)	[2] 2.371(4)	65.01(15)	65.01(16)	9.32	[1] *1.931*	
	2.270(5)						9.72	[2] 1.805	
	2.304	**2.510**	**2.620**	**2.357**	**65.2**	**64.5**			
$[Eu(LS)_3(H_2O)_2]$	2.3729(16)	2.5922(19)	2.7197(18)	[1] 2.4311(16)	64.29(6)	61.92(6)	4.88	[1] 1.729	8.157
	2.3790(16)	2.5823(18)	2.7282(19)	[2] 2.4488(17)	64.10(6)	62.63(6)	1.09	[2] 1.780	
	2.3651(16)						9.67	[2] *2.027*	
	2.372	**2.587**	**2.724**	**2.440**	**64.2**	**62.3**			
$[Gd(LS)_3(H_2O)_2]$	2.352(9)	2.597(11)	2.652(12)	[1] 2.397(8)	64.1(3)	61.7(3)	6.25	[1] 1.791	8.139
	2.359(9)	2.572(11)	2.712(11)	[2] 2.424(8)	64.8(3)	61.9(4)	10.27	[2] 1.737	
	2.338(10)						0.47	[2] *2.113*	
	2.350	**2.585**	**2.682**	**2.411**	**64.5**	**61.8**			
$[Tb(LS)_3(H_2O)_2]$	2.345(3)	2.567(3)	2.701(3)	[1] 2.407(3)	64.76(9)	62.26(9)	5.06	[1] 1.653	8.128
	2.356(2)	2.549(3)	2.711(3)	[2] 2.423(3)	64.75(9)	63.02(9)	9.95	[2] 1.714	
	2.335(2)						1.75	[2] *1.947*	
	2.345	**2.558**	**2.706**	**2.415**	**64.8**	**62.6**			

[a] Each line in the table corresponds to one and the same ligand in the complex (where appropriate). Numbers in bold are averaged data for a complex. [b] N(py) and N(fh) are nitrogen atoms of pyridine and fused heterocycle rings, respectively. [c] Hydrogen bond lengths involving metal-coordinated water molecules. These molecules are labeled as [1] and [2]; the same numbering is used in the column "Ln-OH_2". The lengths of intramolecular H-bonds are shown in italic, and intermolecular ones, in plain text. [d] The shortest metal−metal distance in the structure. [e] Dihedral angle between the planes of pyridine and fused heterocycle. The planes were defined by C, N, O, S atoms of core rings.

always bound to the N and not to the O atom of the benzoxazole ring similarly to the binding scheme reported for $[Ln(NO_3)_3$(2,6-bis(benzoxazolyl)pyridine)],[21] but contrary to [Eu(thenoyltrifluoroacetonate)$_3$(2-(2′-pyridyl)benzoxazole)],[22] in which the ancillary ligand is N,O-chelating. (ii) The Ln-N(pyridine) bond is shorter compared to the Ln-N(fused heterocycle) by 0.055−0.162 Å for benzothiazole, and 0.0154−0.168 Å for benzoxazole. This is indicative of the preference of Ln^{III} ions for the harder carboxylate base compared to the softer N donors, which pulls the metal ion closer to the N(py) donor. (iii) The ligands of the same type within a complex are not equally strongly bonded to the metal ion, as reflected in the different respective sets of bond lengths. This statement applies for the two κ^3-bonded ligands, and the two water molecules in the bis-aqua complexes, and to the three κ^3-bonded ligands in [Eu(κ^3-L)$_3$]. (iv) The κ^1-bonded ligands are more planar in the case of benzothiazole (dihedral angle 0.47−1.75°) compared to benzoxazole (dihedral angle 7.50−14.00°), while for the κ^3-ligands the dihedral angle is $<13°$, irrespective of the nature of the fused heterocycle. (v) The intermolecular metal−metal distance is >8.1 Å, which is likely to prevent significant interaction between metal centers.

The relative bonding strength of the ligands in the 12 analyzed structures can be quantified using the

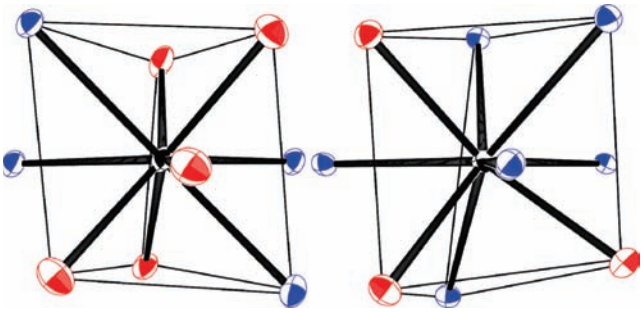

Figure 2. Coordination environment of Eu^{III} in the complexes $[Eu(L)_3(H_2O)_2]$ (left) and $[Eu(L)_3]$ (right). Heteroatoms: O, red; N, blue; Eu, black.

bond-valence method[31] in which a donor atom j in the first coordination sphere lying at a distance $d_{Ln,j}$ from the metal ion is characterized by a bond-valence contribution $v_{Ln,j}$:

$$v_{Ln,j} = e^{(R_{Ln,j} - d_{Ln,j})/b} \quad (1)$$

where $R_{Ln,j}$ are the bond-valence parameters depending on the pair of interacting atoms and which are reported for both Ln-O,[32] and Ln-N[33] bonds, while b is a scaling parameter taken as equal to 0.37 Å for all the interacting pairs of atoms.[31,34] The total bond valence of the lanthanide ion V_{Ln} is simply the sum of the individual $v_{Ln,j}$ contributions, and by definition it is supposed to be equal to the formal oxidation state:

$$V_{Ln} = \sum_j v_{Ln,j} \quad (2)$$

The average total bond valence for the 12 structures is 3.01(7) which reflects their overall good crystallographic quality (Table 2).[32,33] Despite the uncertainties borne by these values, inherent to the model chosen,[32,33] consistent trends are observed in going (i) from the larger Nd^{III} ion to the smaller Tb^{III} ion with a decrease in V_{Ln} from 3.08 to 3.01 for the complexes with L^-, Gd being an exception; (ii) from complexes with L^- to LMe^-, with a decrease of 0.06 on average, and (ii) from complexes with L^- to LS^- with an average decrease of 0.04. Comparison between complexes $[Eu(L)_3]$ and $[Eu(L)_3(H_2O)_2]$ exemplifies a stronger binding of water as compared with pyridine and benzoxazole N atoms, V_{Eu} increasing by 0.09. Looking into more details, the average contributions from the various coordinating groups are remarkably constant and their values are in the expected series, namely, $v(CO_2^-) = 0.41(1) > v(H_2O) = 0.35(1) > v(\text{N-py}) = 0.31(1) > v(\text{N-fh}) = 0.25(2)$, the largest variations being observed for the weakest coordinating group, the nitrogen atom of the fused heterocycle. A significant difference observed between $v(H_2O)$ and v(N-fh) may explain why the ligands tend to form bis-aqua complexes instead of anhydrous ones. Nevertheless, the isolation of $[Eu(\kappa^3\text{-L})_3]$ confirms that anhydrous complexes are accessible, and it remains to be seen if they can be prepared as major products when the synthesis is performed in anhydrous conditions.

^{1}H NMR Spectroscopy of La^{III} Complexes in DMSO-d_6. The resonances of the free deprotonated ligands were determined from the ^{1}H NMR spectra of their salts with the non-coordinating tetraethylammonium cation (Figure 3, Supporting Information, Figures S10−S11, for proton numbering see Scheme 1). These resonances are sharp, resolved at room temperature and shifted upfield compared to those of the protonated ligands, consistent with the negative charge borne by the deprotonated ligands (Supporting Information, Table S1).

The solution behavior of the complexes has been probed on the diamagnetic lanthanum chelates. Since DMSO is known to be a stronger ligand for lanthanides compared to water,[35] the complexes $[Ln(\kappa^3\text{-ligand})_2(\kappa^1\text{-ligand})(H_2O)_2]$ are likely to undergo solvolysis in this solvent to give $[Ln(\kappa^x\text{-ligand})_3(DMSO)_n]$ where x and n will most probably depend on the concentration of the solution.[36]

^{1}H NMR spectra of all studied lanthanum complexes have similar features (Figure 3, Supporting Information, Figures S10−S11) and do not display resonances of non-coordinated protonated or deprotonated ligands. Analyzing the aromatic proton region at room temperature we see that pyridine resonances are very broad and featureless, and are shifted downfield compared to a free ligand anion. At the same time, the resonances of the fused heterocycle are relatively sharp, and are shifted either upfield or downfield with respect to a free deprotonated ligand, for example, for proton *bo*4 the shifts are −0.04 ppm in LMe^-, and +0.13 ppm in LBr^-. For both groups, the extent of the shift depends on the nature of the ligand. These observations confirm that the ligands are indeed coordinated to the lanthanide in DMSO solution.

Considering the mode of binding, clearly, the pyridine ring is coordinated which prevents its free rotation and results in broad resonances; the bonding is likely to be assisted by the presence of a carboxylate group. The broad resonances of pyridine protons may indicate that the ligands undergo exchange, possibly via fluctuation between various κ^x-binding modes. At the same time, the fused heterocycle ring is either not coordinated or only weakly bound, and is free to undergo rotation along the C−C bond connecting it to the pyridine, resulting in sharp resonances. The relative bonding strength of pyridine versus fused heterocycle rings in DMSO is in accord with the results of crystal structure analysis. Upon warming the solutions to 353 K, a single set of sharp and resolved signals is observed for all of the complexes; this is consistent with all three ligands being equivalent on the ^{1}H NMR time scale at that temperature. The observed

(31) Brown, I. D.; Altermatt, D. *Acta Crystallogr., Sect. B* **1985**, *41*, 244.
(32) Trzesowska, A.; Kruszynski, R.; Bartczak, T. J. *Acta Crystallogr., Sect. B* **2004**, *60*, 174.
(33) Trzesowska, A.; Kruszynski, R.; Bartczak, T. J. *Acta Crystallogr., Sect. B* **2005**, *61*, 429.
(34) A recent re-evaluation of the bond-valence method pointed to the parameter b being dependent on both the coordination number and the atomic number: Zocchi, F. *J. Mol. Struct. THEOCHEM* **2007**, *805*, 73; however, re-calculation of the relevant data for the Eu complexes with modified parameters leads to the same values and trends as reflected in Table 2.

(35) (a) Bünzli, J.-C. G.; Yersin, J.-R.; Mabillard, C. *Inorg. Chem.* **1982**, *21*, 1471. (b) Tanaka, F.; Kawasaki, Y.; Yamashita, S. *J. Chem. Soc., Faraday Trans. 1* **1988**, *84*, 1083.(c) Kimura, T.; Nagaishi, R.; Kato, Y.; Yoshida, Z. *J. Alloys Compd.* **2001**, *323−324*, 164.
(36) (a) Bünzli, J.-C. G.; Metabanzoulou, J.-P.; Froidevaux, P.; Jin, L.-P. *Inorg. Chem.* **1990**, *29*, 3875. (b) Milicic-Tang, A.; Bünzli, J.-C. G. *Inorg. Chim. Acta* **1992**, *192*, 201.

Table 2. Calculated Bond Valence Parameters for the Lanthanide Complexes

		$\nu_{Ln,i}(O)$			$\nu_{Ln,i}(N)^a$		
complex	V_{Ln}	CO_2^-	OH_2	average	N(py)	N(fh)	average
$[Nd(L)_3(H_2O)_2]$	3.08	0.42(2)	0.36(1)	0.39(3)	0.30(0)	0.26(3)	0.28(3)
$[Nd(LMe)_3(H_2O)_2]$	3.00	0.40(3)	0.34(1)	0.38(3)	0.30(1)	0.25(2)	0.28(3)
$[Eu(L)_3]$	2.97	0.41(1)		0.41(1)	0.34(3)	0.24(4)	0.29(7)
$[Eu(L)_3(H_2O)_2]$	3.06	0.40(2)	0.36(1)	0.39(3)	0.30(1)	0.26(3)	0.28(3)
$[Eu(LMe)_3(H_2O)_2]$	3.01	0.40(4)	0.34(1)	0.38(4)	0.31(1)	0.25(1)	0.28(4)
$[Eu(LS)_3(H_2O)_2]$	2.96	0.41(1)	0.34(1)	0.38(4)	0.31(1)	0.22(1)	0.28(6)
$[Gd(L)_3(H_2O)_2]$	3.14	0.42(3)	0.37(1)	0.40(4)	0.32(1)	0.26(5)	0.29(4)
$[Gd(LMe)_3(H_2O)_2]$	3.08	0.41(4)	0.34(1)	0.38(5)	0.32(1)	0.27(1)	0.30(3)
$[Gd(LS)_3(H_2O)_2]$	3.07	0.42(1)	0.36(2)	0.40(4)	0.31(1)	0.24(3)	0.27(4)
$[Tb(L)_3(H_2O)_2]$	3.01	0.40(4)	0.35(1)	0.38(4)	0.29(1)	0.26(3)	0.27(3)
$[Tb(LS)_3(H_2O)_2]$	2.95	0.41(1)	0.34(1)	0.38(4)	0.31(1)	0.21(1)	0.26(6)
$[Yb(LBr)_3(H_2O)_2]$	2.89	0.39(3)	0.34(2)	0.37(4)	0.30(1)	0.22(1)	0.26(5)

[a] N(py) and N(fh) are nitrogen atoms of pyridine and fused heterocycle rings, respectively.

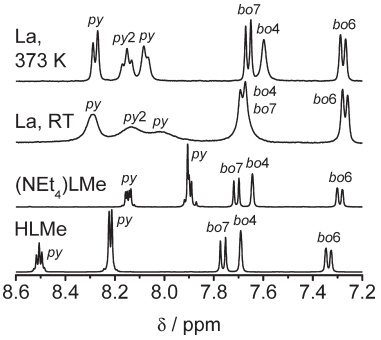

Figure 3. ^{1}H NMR spectra of ligand HLMe, salt $(NEt)_4$LMe, and complex $[La(LMe)_3(H_2O)_2]\cdot H_2O$ (6.30×10^{-4} M) in DMSO-d_6; resonances of pyridine (*py*) and benzoxazole (*bo*) protons are indicated on the plot; for proton numbering see Scheme 1.

changes in the spectra upon heating and cooling are completely reversible.

In conclusion, ^{1}H NMR spectra of the complexes provide evidence that the ligands are coordinated to a lanthanide in DMSO solution. Although the exact mode of binding could not be established from these experiments, we may speculate that it occurs at least via a carboxylate, or via N, O donor atoms of the pyridine-2-carboxylate moiety.

Electronic Spectroscopy. UV−vis absorption spectra of the ligands and their complexes were recorded in DMSO solution at room temperature; they are shown in Figure 4 and Supporting Information, Figures S12−S15, and the main spectral features are summarized in Table 3 and Supporting Information, Table S2. The ligands display a broad absorption band in the UV corresponding to $\pi \rightarrow \pi^*$ transitions with a maximum at 307−314 nm, a shoulder at ≈ 325 nm, and a cut off at ≈ 350 nm. The spectrum of the benzothiazole ligand HLS is red-shifted by 7 nm (700 cm^{-1}) compared to its benzoxazole counterpart HL. Grafting a methyl (in HLMe) or a bromine (in HLBr) onto the benzoxazole ring results in a red shift of about 5 nm (500 cm^{-1}) compared to the parent ligand HL.

No significant changes occur in the shape of the absorption band upon formation of the lanthanide complexes, apart from red shifts of the maximum by up to 4 nm, and of the cutoff which is moved to ≈ 365 nm, and appearance of several shoulders on the red-edge of the band. Additionally, no significant trends are observed in

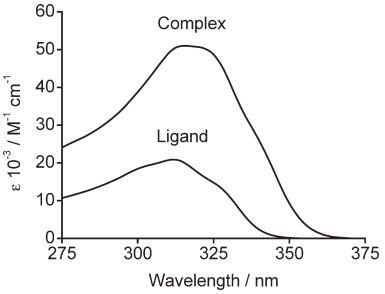

Figure 4. Absorption spectra of ligand HLMe (3.07×10^{-4} M) and complex $[Eu(LMe)_3(H_2O)_2]\cdot H_2O$ (7.75×10^{-5} M) in DMSO solution. Absorption spectra of other ligands and complexes are similar and are provided in the Supporting Information.

Table 3. Absorption Spectra of the Ligands and Their Europium Complexes [a]

	λ_{max}/nm (10^{-3} ε/M^{-1} cm^{-1})		
HLS	314 (20)	$[Eu(LS)_3(H_2O)_2]\cdot 2H_2O$	316 (54)
HL	307 (22)	$[Eu(L)_3(H_2O)_2]\cdot H_2O$	309 (54)
HLMe	312 (21)	$[Eu(LMe)_3(H_2O)_2]\cdot H_2O$	316 (51)
HLBr	311 (21)	$[Eu(LBr)_3(H_2O)_2]\cdot THF$	313 (58)

[a] Spectra were recorded in DMSO solution at room temperature in the spectral range 275−500 nm. Estimated errors are ± 1 nm for λ_{max} and ± 5% for ε. The concentration of the samples was in the range (2.25−3.07) $\times 10^{-4}$ M for the ligands, and (6.72−9.22) $\times 10^{-5}$ M for the Eu^{III} complexes. The absorption spectra of the other lanthanide complexes are similar (Supporting Information, Table S2).

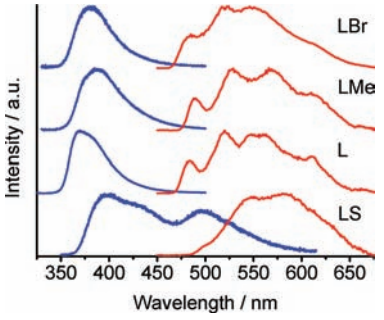

Figure 5. Corrected and normalized fluorescence (blue, 295 K, emission slit − 0.3 nm) and phosphorescence (red, 77 K, emission slit − 7 nm) spectra of gadolinium complexes in solid state.

the electronic spectra as the ion is varied from lanthanum to ytterbium. The absorption coefficients for the complexes are 2.5−3 times higher compared to the free ligands, in line with the formation of 3:1 complexes.

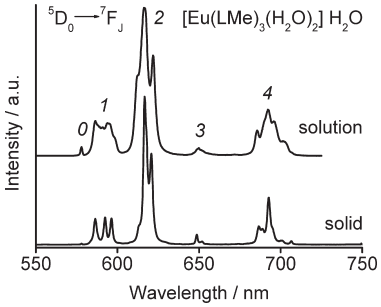

Figure 6. Corrected and normalized luminescence spectra of [Eu(LMe)$_3$(H$_2$O)$_2$]·H$_2$O in solid state and in DMSO solution (2.07×10^{-4} M) at room temperature (emission slit − 0.3 nm). Luminescence transitions of Eu^{III} ($^5D_0 \rightarrow {}^7F_J$, $J = 0-4$) are indicated on the plot. Emission spectra for the other Eu^{III} complexes are similar and are provided in the Supporting Information.

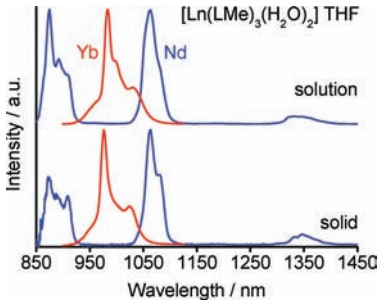

Figure 7. Corrected and normalized luminescence spectra of [Nd(LMe)$_3$(H$_2$O)$_2$]·THF (blue) and [Yb(LMe)$_3$(H$_2$O)$_2$]·THF (red) in solid state (emission slit − 10 nm) and in DMSO solution ($\approx 2 \times 10^{-4}$ M; emission slits are 1.0 nm for Nd^{III}, and 0.2 nm for Yb^{III}) at room temperature. Emission spectra for the other Nd^{III} and Yb^{III} complexes are similar and are provided in the Supporting Information.

Ligand-Centered Luminescence. The energies of the lowest singlet $E(S_1)$ and triplet $E(T_1)$ excited states of the coordinated ligands have been determined from the onset of the luminescence spectra of the Gd^{III} complexes (Figure 5). The corresponding fluorescence spectra were broad and featureless, while phosphorescence spectra showed resolved vibronic structure for 0−0 and 0−1 phonon transitions with progression of ≈ 1500 cm^{-1} (Supporting Information, Table S3), with the exception of [Gd(LS)$_3$(H$_2$O)$_2$]. The determined energies of the singlet and triplet states are: LS^- [$E(S_1/T_1)$ = 27 400/20 400 cm^{-1}], L^- [$E(S_1/T_1)$ = 28700/21 300 cm^{-1}], LMe^- [$E(S_1/T_1)$ = 28 300/21 000 cm^{-1}], and LBr^- [$E(S_1/T_1)$ = 28700/21 400 cm^{-1}]. A large energy gap of 7000−7400 cm^{-1} between the singlet and triplet states is relatively insensitive to the nature of the ligands, and is not ideal for the population of the triplet states.[1] We also note that the values of $E(S_1/T_1)$ follow the trends observed in the absorption spectra of the complexes.

Metal-Centered Luminescence in the Solid State. All of the complexes with luminescent lanthanides were found to emit the characteristic line-like emission of the metal ion in the solid state upon excitation within the absorption band of the ligands as displayed on Figures 6, 7, and Supporting Information, Figures S16−S22. The emission was observed either in the visible (for Eu and Tb) or in the near-infrared (for Nd and Yb), and its intensity was found to depend strongly on the lanthanide ion. Relevant photophysical parameters for the complexes are listed in Tables 4 and 5. The luminescence decays of the excited states are single exponential functions for all of the complexes, pointing to the presence of only one emissive lanthanide center in the solid samples (a similar conclusion has been reached from the analysis of luminescence spectra of europium complexes, see below). The excitation spectra of the europium complexes display a prominent ligand band at < 375 nm, and very weak f-transitions at 395 and 463 nm thus confirming the sensitization of the metal luminescence by the ligands (Supporting Information, Figures S23−S24).

Table 4. Near-Infrared Luminescence Properties of Neodymium and Ytterbium Complexes in Solid State and in DMSO Solution at Room Temperature[a]

complex		$\tau_{obs}/\mu s$	$Q_L^{Ln}/\%$	$Q_{Ln}^{Ln}/\%$[b]	$\eta_{sens}/\%$[b]
[Nd(L)$_3$(H$_2$O)$_2$]·H$_2$O [c]	DMSO	1.83(3)	0.14	0.68	21
[Nd(LMe)$_3$(H$_2$O)$_2$]·THF [c]	DMSO	1.87(1)	0.17	0.69	25
[Nd(LBr)$_3$(H$_2$O)$_2$]·THF [c]	DMSO	1.84(6)	0.11	0.68	16
[Yb(LS)$_3$(H$_2$O)$_2$]·1.5H$_2$O	solid	0.75(5)	0.10		
	DMSO	24(1)	1.00	2.0	50
[Yb(LMe)$_3$(H$_2$O)$_2$]·THF	solid	1.22(5)	0.08		
	DMSO	31(1)	1.25	2.6	49
[Yb(LBr)$_3$(H$_2$O)$_2$]·2H$_2$O	solid	0.65(5)	0.16		
	DMSO	28(1)	1.09	2.3	47

[a] Excitation wavelength was 355 nm for τ_{obs} and 321 or 350 nm for Q_L^{Ln}. Estimated error on Q_L^{Ln} is ± 15%. The concentration of the samples in DMSO solution was $\approx 2 \times 10^{-4}$ M. [b] Q_{Ln}^{Ln} and η_{sens} calculated from eq 3, assuming $\tau_{rad}(Nd)$ = 270 μs[42] and $\tau_{rad}(Yb)$ = 1.2 ms.[40] The errors on their values are of the same magnitude as the errors on τ_{obs} and Q_L^{Ln}, respectively. [c] For Nd^{III} complexes in solid state, $\tau_{obs} < 0.5\ \mu s$ and $Q_L^{Nd} < 0.02\%$.

When it comes to evaluate the emission efficiency of the lanthanide complexes, two main factors are of importance which are described in eq 3, where Q_L^{Ln} and Q_{Ln}^{Ln} are the overall (i.e., measured upon ligand excitation) and intrinsic (i.e., determined upon direct f-f excitation) quantum yields, τ_{obs} is the observed lifetime of the excited state, and τ_{rad} the radiative lifetime, that is the lifetime in absence of non-radiative deactivation processes:

$$Q^{Ln}{}_L = \eta_{sens} \times Q^{Ln}{}_{Ln} = \eta_{sens} \times (\tau_{obs}/\tau_{rad}) \qquad (3)$$

The first factor is the efficiency with which the ligands sensitize the metal-centered luminescence, η_{sens}, which takes into account the energy migration processes occurring both within the ligand and from the ligand to the metal-ion excited states. The second factor, Q_{Ln}^{Ln}, reflects the relative importance of radiative versus non-radiative de-excitation processes operating in the first and, possibly, second coordination spheres of the metal ion. The intrinsic quantum yield of the lanthanide ion is very sensitive to the energy gap between its emitting level and the next available lower energy level since this gap can be bridged by vibrations; the quenching is particularly efficient when high-energy oscillators such as O−H are in the vicinity of the excited metal ion.

The energy gap in the studied ions decreases in the following order: Tb^{III} (14800 cm^{-1}) > Eu^{III} (12 300 cm^{-1}) > Yb^{III} (10 250 cm^{-1}) > Nd^{III} (5300 cm^{-1}).[37] The investigated complexes have two water molecules bound to the lanthanide ion in the solid state, as established from

(37) Carnall, W. T. The absorption and fluorescence spectra of rare earth ions in solution. In *Handbook on the Physics and Chemistry of Rare Earths*; Gschneidner, K. A., Jr., Eyring, L., Eds.; North Holland Publ. Co.: Amsterdam, 1979; Vol. *3*, Chapter 24, pp 171−208, and references therein.

Table 5. Luminescence Properties of Europium Complexes in Solid State and in DMSO Solution at Room Temperature[a]

complex		τ_{obs}/ms	Q_L^{Eu}/%	τ_{rad}/ms[b]	Q_{Eu}^{Eu}/%[b]	η_{sens}/%[b]
$[Eu(LS)_3(H_2O)_2]\cdot 2H_2O$	solid	0.42(1)	13	3.2	13	98
	DMSO	1.39(1)	29	2.7	51	56
$[Eu(L)_3(H_2O)_2]\cdot H_2O$	solid	0.41(1)	12	3.5	12	100
	DMSO	1.97(1)	31	3.6	55	57
$[Eu(LMe)_3(H_2O)_2]\cdot H_2O$	solid	0.47(5)	14	3.3	14	97
	DMSO	2.00(3)	39	3.7	54	72
$[Eu(LBr)_3(H_2O)_2]\cdot THF$	solid	0.46(5)	13	3.5	13	98
	DMSO	1.73(3)	29	3.6	48	60

[a] Excitation wavelength was 355 nm for τ_{obs} and 321 nm for Q_L^{Eu}. Estimated error on Q_L^{Eu} is ± 15%. The concentration of the samples in DMSO solution was $\approx 2 \times 10^{-4}$ M. [b] Q_{Eu}^{Eu}, η_{sens} and τ_{rad} calculated from eqs 3 and 4. For solid state samples, a refractive index $n = 1.5$ was assumed. The errors on Q_{Eu}^{Eu} and η_{sens} are of the same magnitude as the errors on τ_{obs} and Q_L^{Eu}, respectively.

the X-ray structural studies, which renders them amenable to quenching by O−H vibrations, particularly in the case of the NIR-emitting ions. This is confirmed by the very short excited state lifetimes, and low sensitized quantum yields found for the complexes of Nd^{III} (< 0.5 μs, < 0.02%) and Yb^{III} (0.65−1.22 μs, 0.08−0.16%). As a matter of fact, anhydrous organic complexes of these ions usually display $\tau_{obs} > 1$ μs (Nd),[4,24,38] and > 5 μs (Yb).[4,39]

In the case of europium complexes, which emit in the visible, the photophysical parameters are also consistent with the presence of coordinated water. It is reflected in a short luminescence lifetime of europium (0.41−0.47 ms) which is temperature independent: for instance $\tau_{obs}(10K) =$ 0.44(1) ms for $[Eu(LMe)_3(H_2O)_2]\cdot H_2O$, as compared to 0.47(5) ms at 295 K. Nevertheless, europium complexes in the solid state display sizable sensitized luminescence yields of 12−14% (Table 5). Attempts to experimentally determine intrinsic quantum yields of Eu^{III} upon excitation within f-f transitions failed because of very low absorption intensity. Fortunately, the radiative lifetime of $Eu(^5D_0)$ can be calculated from the simple treatment of its corrected emission spectrum according to eq 4, where n is the refractive index of the medium, $A_{MD,0}$ is the spontaneous emission probability for the $^5D_0 \rightarrow {}^7F_1$ transition in vacuo, calculated to be equal to 14.65 s^{-1}, and I_{tot}/I_{MD} is the ratio of the total area of the corrected Eu^{III} emission spectrum to the area of the magnetic dipole $^5D_0 \rightarrow {}^7F_1$ transition.[40]

$$1/\tau_{rad} = A_{MD,0} \times n^3 \times (I_{tot}/I_{MD}) \qquad (4)$$

When $n = 1.5$ is assumed for solid state metal-organic complexes, the calculated radiative lifetime falls into the narrow range 3.2−3.5 ms for all four complexes, in line with the similar O_5N_4 coordination environment around europium. More interesting, the calculated sensitization efficiency of the europium luminescence by the ligands in the solid is close to unity (eq 3, Table 5).

The luminescence spectra of europium complexes are very similar (Figures 6 and Supporting Information, Figures S16−S22, Table S4) and will be discussed in detail for $[Eu(LMe)_3(H_2O)_2]\cdot H_2O$ only. The luminescence lines originating from the $Eu(^5D_0)$ excited level are sharp and can be analyzed under high resolution conditions in terms of local symmetry of the metal ion (Supporting Information, Figures S25−S26, Table S5). The $^5D_0 \rightarrow {}^7F_0$ transition, which is expected to provide a single line for a single coordination environment, does effectively display only one, symmetrical component of weak intensity at 17 271 cm^{-1}, with a ratio $I(^7F_0)/I(^7F_1) =$ 0.008 (Supporting Information, Table S4). The $^5D_0 \rightarrow {}^7F_1$ transition contains three components of equal intensity, corresponding to $^7F_1$ crystal-field sublevels located at 237, 419, and 524 cm^{-1} above $^7F_0$ (Figures 6, Supporting Information, Figure S26, Table S5). When the europium ion resides in a coordination site with low symmetry, these components should be equally spaced; this is not quite the case here since $\Delta E = 182$ and 105 cm^{-1}, reflecting the trace of a pseudo-trigonal symmetry, consistent with the distorted tricapped trigonal prismatic coordination polyhedron seen in the crystal structure. This conclusion is further backed by the hypersensitive $^5D_0 \rightarrow {}^7F_2$ transition which dominates the spectrum with $I(^7F_2)/I(^7F_1) = 3.6$, and consequently excluding the presence of an inversion center.

The complexes of terbium display green luminescence (Supporting Information, Figures S22) but its efficiency in solid state at room temperature is very low (< 0.02%). The emissive state of Tb^{III} ($^5D_4$: 20 500 cm^{-1})[37] is isoenergetic with the triplet states of the ligands and is likely to be quenched by back energy transfer.[41] In view of this finding, terbium complexes were not investigated any further.

Metal-Centered Luminescence in DMSO Solution. The luminescence properties of the complexes have also been studied in dilute DMSO solutions (ca. 2×10^{-4} M) in which DMSO is expected to displace the quenching water molecules from the inner coordination sphere, as discussed earlier, leading to improved emissive properties. The luminescence spectra of the complexes in DMSO are much broader compared to in the solid state and have an altered intensity ratio of emission bands which also points to their solvolysis (Figures 6−7 and Supporting Information, Figures S16−S21). In the case of Eu^{III}, this broadening renders difficult the analysis of the fine structure. However, more than three bands are observed for the $^5D_0 \rightarrow {}^7F_1$ transition evidencing the presence of several emitting species in solution. Although we cannot specify

(38) Shavaleev, N. M.; Scopelliti, R.; Gumy, F.; Bünzli, J.-C. G. *Inorg. Chem.* **2008**, *47*, 9055.
(39) Tsvirko, M. P.; Meshkova, S. B.; Venchikov, V. Ya.; Topilova, Z. M.; Bol'shoi, D. V. *Opt. Spectrosc. (Engl. Transl.)* **2001**, *90*, 669.
(40) (a) Werts, M. H. V.; Jukes, R. T. F.; Verhoeven, J. W. *Phys. Chem. Chem. Phys.* **2002**, *4*, 1542. (b) Aebischer, A.; Gumy, F.; Bünzli, J.-C. G. *Phys. Chem. Chem. Phys.* **2009**, *11*, 1346.
(41) Latva, M.; Takalo, H.; Mukkala, V.-M.; Matachescu, C.; Rodriguez-Ubis, J. C.; Kankare, J. *J. Lumin.* **1997**, *75*, 149.
(42) Weber, M. J. *Phys. Rev.* **1968**, *171*, 283.

which of the complexes [Ln(κ^x-ligand)$_3$·*n*DMSO] dominate in solution (*x* and *n* are unknown), we note that the luminescence decays of all the samples are single exponential functions at room temperature, suggesting that these species are in equilibrium on the time scale of the excited state lifetime. The data reported in Tables 4 and 5 represent therefore averages with respect to the solution composition.

When the DMSO solution of Eu^{III} complex with LMe^- is frozen to 10 K, the high-resolution scan of the $^5D_0 \rightarrow {}^7F_1$ transition shows the presence of at least three species. Two of these species contribute >90% to emission intensity of the band, and are likely to be anhydrous, while the third species contribute <10% (Supporting Information, Figure S26). The $^5D_0 \rightarrow {}^7F_0$ transition at 10 K is effectively a single band, although somewhat asymmetric on its high-energy side, broadened (fwhh = 25 cm^{-1}) with respect to the solid state sample (15 cm^{-1}), and red-shifted by about 10 cm^{-1}. Under the same experimental conditions (10 K), the Eu($^5D_0$) excited state decay becomes bi-exponential, a result of the "freezing" of the equilibrium; the long lifetime, 2.01(5) ms, with relative population of 88% corresponds to the anhydrous species, while the shorter, 0.54(6) ms with population of 12%, is diagnostic of the species with coordinated water molecule(s).

For europium complexes at room temperature, a significant improvement in the luminescence properties is observed in DMSO solution compared to the solid samples, which is consistent with the formation of anhydrous species. The measured quantum yield and lifetime increase to 29−39% and 1.39−2.0 ms, respectively (Table 5). Use of eq 4 with $n = 1.4785$ for DMSO, yields $\tau_{rad} = 2.6$ ms for the benzothiazole complex and $\tau_{rad} = 3.6-3.7$ ms for benzoxazole complexes; from these values, the intrinsic quantum yields $Q_{Eu}^{Eu} = 48-55\%$, and sensitization efficiencies ($\eta_{sens} = 56-72\%$) can be calculated. The drop in ligand-to-europium sensitization efficiency in solution compared to the solid state might be attributed to the change of the binding mode of the ligand in DMSO which was postulated when discussing ^{1}H NMR spectra.

In DMSO, the emissive properties of the Nd^{III} and Yb^{III} complexes are closer to those reported for anhydrous species.[4,24,38,39] The experimentally determined photophysical parameters, τ_{obs} and Q_L^{Ln}, increase to 1.83−1.87 μs and 0.11−0.17% for neodymium, and 24−31 μs and 1.00−1.25% for ytterbium, respectively (Table 4). The intrinsic quantum yields Q_{Ln}^{Ln} calculated from eq 3, and assuming $\tau_{rad}(Nd) = 270$ μs[42] and $\tau_{rad}(Yb) = 1.2$ ms,[40] also increase to 0.68−0.69% for Nd^{III} and 2.0−2.6% for Yb^{III}. In DMSO, the ligand sensitizes ytterbium luminescence with calculated $\eta_{sens} \approx 50\%$, while η_{sens} for neodymium is much smaller, 16−25%. However, the reported range for $\tau_{rad}(Nd)$ is broad (0.3−3 ms),[4] and the value we used may not be completely appropriate for its organic complexes.

Conclusions

We have introduced two new classes of tridentate ligands based on benzothiazole- and benzoxazole-substituted pyridine-2-carboxylic acids and developed their facile synthesis from simple starting materials. The ligands form mononuclear nine-coordinate complexes [Ln(κ^3-ligand)$_2$(κ^1-ligand)(H_2O)$_2$] with light and heavy lanthanides, and sensitize their luminescence in the visible and the near-infrared. The following statements can be made considering the reported photophysical data.

(i) With respect to a given lanthanide ion, all four ligands investigated in this work provide complexes with similar photophysical parameters. No particular beneficial effect of a heavy bromine atom on the lanthanide luminescence is observed with ligand LBr^-, while electron-donating methyl group in ligand LMe^- is found to improve somewhat the luminescence of a metal center.[24]

(ii) Benzothiazole- and benzoxazole-substituted pyridine-2-carboxylates are adequate sensitizers for europium. Indeed, their excited states lie at sufficiently higher energy compared to the $^5D_0$ state to avoid back energy transfer. In addition, neither of the benzothiazole- nor benzoxazole-pyridine groups are electron-rich,[44] so that electron-transfer quenching is unlikely to be important in their europium complexes.[45] As a result, even in the presence of two metal-bound water molecules, the quantum yields of the sensitized Eu^{III} luminescence are sizable, up to 14%.

(iii) The introduction of a benzothiazole instead of a benzoxazole in the ligand HLS versus HL results in a red shift in the energy of its first singlet and triplet excited states by 1300 cm^{-1} and 900 cm^{-1}, respectively. The photophysical properties of the corresponding Eu^{III} complexes are however similar, apart from a shorter luminescence lifetime for the benzothiazole complex. It may be explained by the lower energy of the triplet state and a resulting higher probability of back energy transfer.[41]

(iv) The low energy of the triplet state in the new ligands (<21 400 cm^{-1}) limits their application as sensitizers for terbium because of the competing back energy transfer.[41]

(v) Although the ligands sensitize near-infrared luminescence of neodymium and ytterbium, coordinated water molecules and proximate C−H oscillators quench excited states of these ions and limit their emission efficiency.[43] On removal of the bound water, the photophysical parameters of Nd^{III} and Yb^{III} complexes improve substantially.

Future studies with these ligands will include synthesis of their anhydrous lanthanide complexes, their application as small-molecule sensitizers in lanthanide-doped nanoparticles,[46] and incorporation in polydentate ligands as chelating and chromophoric units.

Experimental Section

General Methods, Equipment, and Chemicals Used. Elemental analyses were performed by Dr. E. Solari, Service for Elemental Analysis, Institute of Chemical Sciences and Engineering (EPFL). Absorption spectra were measured on a Perkin-Elmer Lambda 900 UV/vis/NIR spectrometer; ^{1}H NMR spectra (presented as δ in ppm and *J* in Hz) were recorded on a Bruker Avance DRX 400 MHz spectrometer. Luminescence emission spectra were measured on a Fluorolog FL 3-22

(43) Yanagida, S.; Hasegawa, Y.; Murakoshi, K.; Wada, Y.; Nakashima, N.; Yamanaka, T. *Coord. Chem. Rev.* **1998**, *171*, 461.
(44) (a) Czerwieniec, R.; Kapturkiewicz, A.; Lipkowski, J.; Nowacki, J. *Inorg. Chim. Acta* **2005**, *358*, 2701. (b) Richardson, C.; Keene, F. R.; Steel, P. J. *Aust. J. Chem.* **2008**, *61*, 183.
(45) Napier, G. D. R.; Neilson, J. D.; Shepherd, T. M. *Chem. Phys. Lett.* **1975**, *31*, 328.
(46) (a) Charbonnière, L. J.; Rehspringer, J.-L.; Ziessel, R.; Zimmermann, Y. *New J. Chem.* **2008**, *32*, 1055. (b) Zhang, J.; Shade, C. M.; Chengelis, D. A.; Petoud, S. *J. Am. Chem. Soc.* **2007**, *129*, 14834.

spectrometer from Horiba-Jobin Yvon-Spex equipped for both visible and NIR measurements. Quantum yield data were determined on the same instrument through an absolute method using a home-modified integrating sphere[40b] with estimated error ±15%. Luminescence lifetimes were measured with a previously described instrumental setup.[38] All luminescence spectra were corrected for the instrumental function. Spectroscopic studies were conducted in solutions in DMSO (Fluka, >99.9%, ACS spectrophotometric grade) freshly prepared before each experiment using optical cells of 2 mm path length; solid state samples were put into 2 mm i.d. quartz capillaries. All spectroscopic measurements were conducted with the samples of lanthanide complexes obtained directly from the synthesis and used without further purification. Absorption spectra were recorded at room temperature in the spectral range 275−500 nm. Estimated errors are ±1 nm for λ_{max} and ± 5% for ε. The concentration of the samples was in the range $(2.25-3.07) \times 10^{-4}$ M for the ligands, and $(4.18-9.22) \times 10^{-5}$ M for the complexes.

Chemicals obtained from commercial suppliers were used without further purification: SeO_2 (99.8%, Acros), DMSO (Acros, 99.7%, extra dry, over mol. sieve, water < 50 ppm). Chromatography was performed on a column with an i.d. of 30 mm using silica gel 60 for preparative chromatography (Fluka, Nr 60752). The progress of reactions and elution of products was followed on TLC plates (silica gel 60 F_{254} on aluminum sheets, Merck).

X-ray Crystallography. The crystal data and structure refinement parameters are presented in Table 6. To grow crystals for X-ray analysis, a small batch (1−2 mg) of the complex was dissolved in a small volume (1−3 mL) of boiling CH_3CN or ethanol followed by cooling and slow evaporation of the solution for 1−4 weeks under air in the dark. Data collections for the 12 crystal structures were performed at low temperature (100 or 140 K) using Mo K_α radiation. An Oxford Diffraction Sapphire/KM4 CCD was employed for Gd^{III} complexes while the remaining samples were measured on a Bruker APEX II CCD. Both diffractometers had a kappa geometry goniometer. Data were reduced by means of CrysAlis PRO[47] for Gd^{III} complexes, and EvalCCD[48] for the remaining samples, and then corrected for absorption.[49] Solution and refinement for all crystal structures were performed by SHELX.[50] All structures were refined using full-matrix least-squares on F^2 with all non-hydrogen atoms anisotropically defined. Hydrogen atoms were placed in calculated positions by means of the "riding" model. In the case of $[Ln(L)_3(H_2O)_2]$ (Ln: Gd, Tb), solvent molecules were disordered and were treated by means of the split model and by applying some restraints or constraints to their coordinates or displacement parameters. Twinning problems by reticular merohedry were discovered in the case of $[Nd(L)_3(H_2O)_2]$ and $[Gd(LS)_3(H_2O)_2]$. The twinning was analyzed by the TWINROTMAT routine of PLATON;[51] a HKLF5 file was then generated and used in the final stages of refinement of the two structures.

Synthesis of 2-Pyridinecarboxaldehyde-6-Methanol. The reaction was performed under nitrogen. 2,6-Pyridinedimethanol (Acros or Aldrich, 1 g, 7.19 mmol, small excess) and SeO_2 (0.395 g, 3.56 mmol) were suspended in dioxane (20 mL, neither dried nor degassed) at room temperature. The reaction mixture was stirred at 65 °C for 48 h to give a colorless solution containing a black precipitate of Se (the reaction mixture was sonicated after 24 h of stirring to break up lumps of precipitated Se). It was cooled to room temperature, diluted with CH_2Cl_2, filtered through Celite, and washed with CH_2Cl_2. Combined filtrates were evaporated to dryness to give yellow oil which was purified immediately to avoid formation of an insoluble solid. Purification was achieved by chromatography (> 15 g of silica). Elution with CH_2Cl_2 removed the byproduct 2,6-pyridinedicarboxaldehyde, followed by elution with 2.5% of CH_3OH in CH_2Cl_2 to recover the product. The product was obtained as a pale yellow oil which after standing overnight solidified to a white solid. While the oil is soluble in organic solvents, the solid is insoluble in most organic solvents or dissolves very slowly. ^{1}H NMR spectra of the solid recorded in $CDCl_3$ or DMSO-d_6 were not informative. It is likely that the product undergoes reversible polymerization in the solid phase. This polymerization does not influence its reactivity apart from slower dissolution. The product shows a single spot on TLC (silica, ethyl acetate). White solid: 754−800 mg ($C_7H_7NO_2$; MW 137.14; 5.50−5.83 mmol, 76−81%). This synthetic procedure is amenable to scale-up without loss in the yield.

Synthesis of Pyridine-2-Carboxylic Acids. The reactions were performed under air. An aldehyde precursor (see Supporting Information) was dissolved in formic acid at room temperature to a give yellow solution which sometimes appeared as being cloudy because of the presence of a red solid, probably, residual Se from the previous synthetic step. The amount of formic acid was chosen to correspond either to a minimum of 3−5 mol equiv relative to aldehyde or to the minimum volume necessary to dissolve the aldehyde at 0 °C. This solution was cooled to 0 °C and cold H_2O_2 was added in excess. The solution was stirred and occasionally sonicated at 0 °C for 4−6 h, and kept overnight at 0 °C (for HL and HLBr the product may precipitate as a white solid in the course of reaction). Ice-cold water was added dropwise at 0 °C to the reaction mixture to precipitate the product. The resulting suspension was stirred at 0 °C for 1−2 h and filtered to give a white solid. It was thoroughly washed with water and suitable organic solvent and dried under vacuum. In the description of ^{1}H NMR spectra, the pyridine, and benzothiazole or benzoxazole protons are labeled as *py*, and *bt* or *bo*, respectively; for proton numbering see Scheme 1. Further details are provided below.

HLS. The reaction was performed with LS-CHO (526 mg, 2.19 mmol), formic acid (35 mL, 42.7 g, 0.93 mol) and H_2O_2 (1.1 mL of 30% wt. aq. solution, contains 330 mg of H_2O_2, 9.70 mmol). The product was precipitated with water (20 mL), and washed with water and ether. White solid: 443 mg (1.73 mmol, 79%). Anal. Calcd for $C_{13}H_8N_2O_2S$ (MW 256.28): C, 60.93; H, 3.15; N, 10.93. Found: C, 60.55; H, 3.18; N, 10.95. ^{1}H NMR (400 MHz, DMSO-d_6): 8.56−8.48 (*py*, m, 1H), 8.26−8.15 (*py* + {*bt*4 or *bt*7}, m, 3H), 8.13 (*bt*4 or *bt*7, d, J 8.0, 1H), 7.59 (*bt*5 or *bt*6, t, J 7.2, 1H), 7.53 (*bt*5 or *bt*6, t, J 7.2, 1H), CO_2H not observed.

HL. The reaction was performed with L-CHO (285 mg, 1.27 mmol), formic acid (3.4 mL, 4.15 g, 90 mmol) and H_2O_2 (0.6 mL of 30% wt. aq. solution, contains 180 mg of H_2O_2, 5.29 mmol). The product was precipitated with water (5 mL), and washed with water and ether. White solid: 256 mg (1.07 mmol, 84%). Anal. Calcd for $C_{13}H_8N_2O_3$ (MW 240.21): C, 65.00; H, 3.36; N, 11.66. Found: C, 64.34; H, 3.36; N, 11.24. ^{1}H NMR (400 MHz, DMSO-d_6): 8.56−8.49 (*py*, m, J 4.4, 1H), 8.26−8.20 (*py*, m, 2H), 7.94−7.88 (*bo*4 + *bo*7, m, 2H), 7.53 (*bo*5 or *bo*6, t, J 7.2, 1H), 7.48 (*bo*5 or *bo*6, t, J 7.2, 1H), CO_2H not observed.

HLMe. The reaction was performed with LMe-CHO (370 mg, 1.55 mmol), formic acid (4 mL, 4.88 g, 0.11 mol) and H_2O_2 (0.8 mL of 30% wt. aq. solution, contains 240 mg of H_2O_2, 7.06 mmol). The product was precipitated with water (9 mL), and washed with water and hexane. White solid: 253 mg (1.00 mmol, 64%). Anal. Calcd for $C_{14}H_{10}N_2O_3$ (MW 254.24): C, 66.14; H, 3.96; N, 11.02. Found: C, 66.29; H, 3.96; N, 10.67.

(47) *CrysAlis PRO*; Oxford Diffraction Ltd.: Yarnton, Oxfordshire, U.K., 2008.
(48) Duisenberg, A. J. M.; Kroon-Batenburg, L. M. J.; Schreurs, A. M. M. *J. Appl. Crystallogr.* **2003**, *36*, 220.
(49) Blessing, R. H. *Acta Crystallogr., Sect. A* **1995**, *51*, 33.
(50) Sheldrick, G. M. *Acta Crystallogr., Sect. A* **2008**, *64*, 112.
(51) Spek, A. L. *J. Appl. Crystallogr.* **2003**, *36*, 7.

Table 6. Crystal Data and Structure Refinement[a]

compound	$[Nd(L)_3(H_2O)_2]$	$[Eu(L)_3(H_2O)_2]$	$[Eu(L)_3]$	$[Gd(L)_3(H_2O)_2]$	$[Tb(L)_3(H_2O)_2]$	$[Nd(LMe)_3(H_2O)_2]$
recryst solvent	CH_3CN	CH_3CN	C_2H_5OH	CH_3CN	C_2H_5OH	CH_3CN
empirical formula	$C_{39}H_{25}N_6NdO_{11}\cdot CH_3CN$	$C_{39}H_{25}EuN_6O_{11}\cdot CH_3CN$	$C_{39}H_{21}EuN_6O_9\cdot 2C_2H_5OH$	$C_{39}H_{25}GdN_6O_{11}\cdot CH_3CN$	$C_{39}H_{25}N_6O_{11}Tb\cdot C_2H_5OH$	$C_{42}H_{31}N_6NdO_{11}\cdot CH_3CN$
fw	938.94	946.66	961.71	951.95	958.64	981.02
temp [K]	100(2)	100(2)	100(2)	140(2)	100(2)	100(2)
cryst syst	triclinic	triclinic	monoclinic	triclinic	triclinic	monoclinic
space group	$P\bar{1}$	$P\bar{1}$	$P2_1/c$	$P\bar{1}$	$P\bar{1}$	$P2_1/c$
unit cell dimensions	a = 12.0867(17) Å	a = 12.0607(16) Å	a = 12.3155(14) Å	a = 12.0406(18) Å	a = 12.0475(9) Å	a = 15.131(16) Å
	b = 14.2706(15) Å	b = 14.1810(17) Å	b = 26.6467(16) Å	b = 14.148(2) Å	b = 14.2135(14) Å	b = 14.516(14) Å
	c = 14.2725(12) Å	c = 14.2411(17) Å	c = 13.1243(9) Å	c = 14.241(2) Å	c = 14.3165(17) Å	c = 18.853(11) Å
	α = 60.381(8)°	α = 60.387(9)°	α = 90°	α = 60.644(15)°	α = 62.953(8)°	α = 90°
	β = 89.928(9)°	β = 66.353(9)°	β = 116.734(6)°	β = 66.243(14)°	β = 65.169(5)°	β = 96.86(7)°
	γ = 66.592(10)°	γ = 89.641(9)°	γ = 90°	γ = 89.518(12)°	γ = 89.534(7)°	γ = 90°
vol [Å]^3	1904.3(4)	1882.6(4)	3846.6(6)	1880.1(5)	1930.2(3)	4111(6)
Z	2	2	4	2	2	4
ρ (calc) [Mg/m^3]	1.637	1.670	1.661	1.682	1.649	1.585
μ [mm^{-1}]	1.437	1.741	1.704	1.839	1.906	1.335
F(000)	942	948	1936	950	960	1980
cryst size [mm^3]	0.38 × 0.19 × 0.17	0.28 × 0.23 × 0.22	0.22 × 0.17 × 0.10	0.14 × 0.14 × 0.12	0.24 × 0.21 × 0.20	0.22 × 0.18 × 0.08
θ range	3.37−27.52°	3.38−27.50°	3.40−27.52°	2.84−26.02°	3.30−27.50°	3.35−25.03°
index ranges	$-15 \le h \le 15$	$-15 \le h \le 15$	$-15 \le h \le 15$	$-14 \le h \le 14$	$-15 \le h \le 15$	$-17 \le h \le 18$
	$-15 \le k \le 18$	$-18 \le k \le 18$	$-34 \le k \le 34$	$-17 \le k \le 17$	$-18 \le k \le 18$	$-16 \le k \le 17$
	$-18 \le l \le 18$	$-18 \le l \le 18$	$-17 \le l \le 17$	$-17 \le l \le 17$	$-18 \le l \le 18$	$-22 \le l \le 22$
reflns collected	8689	40039	93628	16709	42737	51245
independent reflns	8689 [R(int) = 0.0000]	8599 [R(int) = 0.0651]	8828 [R(int) = 0.0420]	7354 [R(int) = 0.1491]	8841 [R(int) = 0.0310]	7203 [R(int) = 0.2462]
completeness to θ	27.52° − 99.1%	27.50° − 99.4%	27.52° − 99.6%	26.02° − 99.3%	27.50° − 99.5%	25.03° − 99.4%
max/min transm	1.0000/0.7973	1.0000/0.6679	1.0000/0.8686	1.00000/0.74604	1.0000/0.8814	1.0000/0.3857
data/restraints/params	8689/72/583	8599/6/564	8828/0/550	7354/300/581	8841/56/585	7203/7/580
GOF on F^2	1.237	1.196	1.101	0.855	1.142	1.073
final R indices [$I > 2\sigma(I)$]	R1 = 0.0656	R1 = 0.0435	R1 = 0.0222	R1 = 0.0788	R1 = 0.0234	R1 = 0.1107
	wR2 = 0.1841	wR2 = 0.1134	wR2 = 0.0440	wR2 = 0.1105	wR2 = 0.0494	wR2 = 0.2494
R indices (all data)	R1 = 0.0804	R1 = 0.0509	R1 = 0.0288	R1 = 0.1725	R1 = 0.0305	R1 = 0.1944
	wR2 = 0.1923	wR2 = 0.1187	wR2 = 0.0462	wR2 = 0.1313	wR2 = 0.0523	wR2 = 0.2991
largest diff. peak/hole [e/Å^3]	3.123/−1.615	2.720/−1.249	0.581/−0.339	1.675/−0.946	0.759/−0.652	2.258/−1.789

compound	$[Eu(LMe)_3(H_2O)_2]$	$[Gd(LMe)_3(H_2O)_2]$	$[Yb(LBr)_3(H_2O)_2]$	$[Eu(LS)_3(H_2O)_2]$	$[Gd(LS)_3(H_2O)_2]$	$[Tb(LS)_3(H_2O)_2]$
recryst solvent	CH_3CN	C_2H_5OH	CH_3CN	C_2H_5OH	C_2H_5OH	C_2H_5OH
empirical formula	$C_{42}H_{31}EuN_6O_{11}\cdot CH_3CN$	$C_{42}H_{31}GdN_6O_{11}\cdot C_2H_5OH$	$C_{39}H_{22}Br_3N_6O_{11}Yb\cdot CH_3CN$	$C_{39}H_{25}EuN_6O_8S_3\cdot C_2H_5OH\cdot H_2O$	$C_{39}H_{25}GdN_6O_8S_3\cdot C_2H_5OH\cdot H_2O$	$C_{39}H_{25}N_6O_8S_3Tb\cdot C_2H_5OH\cdot H_2O$
fw	988.74	999.05	1204.45	1017.87	1023.16	1024.83
temp [K]	100(2)	140(2)	100(2)	100(2)	140(2)	100(2)
cryst syst	monoclinic	monoclinic	monoclinic	triclinic	triclinic	triclinic
space group	$P2_1/c$	$P2_1/c$	$P2_1/c$	$P\bar{1}$	$P\bar{1}$	$P\bar{1}$
unit cell dimensions	a = 15.086(7) Å	a = 15.0055(2) Å	a = 15.0118(19) Å	a = 12.1822(16) Å	a = 12.1389(18) Å	a = 12.1594(12) Å
	b = 14.565(4) Å	b = 14.8825(3) Å	b = 14.560(2) Å	b = 14.6625(14) Å	b = 14.609(2) Å	b = 14.6122(19) Å
	c = 18.677(5) Å	c = 18.4058(4) Å	c = 18.4450(15) Å	c = 14.8430(14) Å	c = 14.7884(19) Å	c = 14.7852(17) Å
	α = 90°	α = 90°	α = 90°	α = 118.006(7)°	α = 118.006(7)°	α = 12.1389(18)
	β = 96.87(2)°	β = 94.8449(17)°	β = 96.266(8)°	β = 91.984(8)°	β = 91.869(11)°	β = 91.976(8)°
	γ = 90°	γ = 90°	γ = 90°	γ = 112.457(8)°	γ = 112.461(15)°	γ = 112.547(7)°
vol [Å]^3	4075(2)	4095.68(13)	4007.6(9)	2087.6(4)	2067.7(5)	2071.1(4)
Z	4	4	4	2	2	2
ρ (calc) [Mg/m^3]	1.612	1.620	1.996	1.619	1.643	1.643
μ [mm^{-1}]	1.612	1.693	5.398	1.718	1.821	1.925

Table 6. Continued

compound	[Eu(LMe)$_3$(H$_2$O)$_2$]	[Gd(LMe)$_3$(H$_2$O)$_2$]	[Yb(LBr)$_3$(H$_2$O)$_2$]	[Eu(LS)$_3$(H$_2$O)$_2$]	[Gd(LS)$_3$(H$_2$O)$_2$]	[Tb(LS)$_3$(H$_2$O)$_2$]
F(000)	1992	2012	2332	1024	1026	1028
cryst size [mm^3]	0.21 × 0.16 × 0.14	0.39 × 0.34 × 0.24	0.20 × 0.17 × 0.17	0.27 × 0.24 × 0.16	0.15 × 0.14 × 0.12	0.21 × 0.14 × 0.14
θ range	3.35−26.83°	2.72−26.37°	3.33−27.50°	3.31−27.50°	2.76−26.02°	3.31−27.50°
index ranges	$-19 \le h \le 19$	$-18 \le h \le 18$	$-19 \le h \le 19$	$-15 \le h \le 15$	$-14 \le h \le 14$	$-15 \le h \le 15$
	$-18 \le k \le 18$	$-18 \le k \le 18$	$-18 \le k \le 18$	$-19 \le k \le 19$	$-18 \le k \le 17$	$-18 \le k \le 18$
	$-23 \le l \le 23$	$22 \le l \le 21$	$-23 \le l \le 23$	$-19 \le l \le 19$	$-18 \le l \le 18$	$-19 \le l \le 19$
reflns collected	67116	35121	87172	49865	8082	50589
independent reflns	8710 [R(int) = 0.1863]	8321 [R(int) = 0.0380]	9191 [R(int) = 0.0879]	9559 [R(int) = 0.0350]	8082 [R(int) = 0.0000]	9480 [R(int) = 0.0663]
completeness to θ	26.83° − 99.5%	26.37° − 99.2%	27.50° − 99.8%	27.50° − 99.7%	26.02° − 99.2%	27.50° − 99.7%
max/min transm	1.0000/0.3727	1.00000/0.84806	1.0000/0.7641	1.0000/0.8680	1.00000/0.87190	1.0000/0.8702
data/restraints/params	8710/7/580	8321/7/585	9191/11/580	9559/18/568	8082/357/569	9480/18/568
GOF on F^2	1.108	1.278	1.205	1.105	0.758	1.126
final R indices [$I > 2\sigma(I)$]	R1 = 0.1129	R1 = 0.0523	R1 = 0.0504	R1 = 0.0234	R1 = 0.0828	R1 = 0.0385
	wR2 = 0.2301	wR2 = 0.1132	wR2 = 0.0871	wR2 = 0.0536	wR2 = 0.0816	wR2 = 0.0731
R indices (all data)	R1 = 0.2011	R1 = 0.0624	R1 = 0.0778	R1 = 0.0273	R1 = 0.2859	R1 = 0.0489
	wR2 = 0.2747	wR2 = 0.1162	wR2 = 0.0964	wR2 = 0.0555	wR2 = 0.1157	wR2 = 0.0771
largest diff. peak/hole [e/Å^3]	3.892/−1.840	3.134/−0.845	1.913/−1.049	0.632/−0.754	0.985/−1.065	1.007/−1.070

[a] Data in common: Wavelength − 0.71073 Å. Refinement method − full-matrix least-squares on F^2. Absorption correction: semiempirical from equivalents.

^{1}H NMR (400 MHz, DMSO-d$_6$): 8.54−8.47 (*py*, m, 1H), 8.26−8.16 (*py*, m, 2H), 7.76 (*bo*7, d, J 8.4, 1H), 7.69 (*bo*4, s, 1H), 7.34 (*bo*6, d, J 8.4, 1H), 2.48 (s, 3H), CO_2H not observed.

HLBr. The reaction was performed with LBr-CHO (414 mg, 1.37 mmol), formic acid (20 mL, 24.4 g, 0.53 mol) and H_2O_2 (0.8 mL of 30% wt. aq. solution, contains 240 mg of H_2O_2, 7.06 mmol). The product was precipitated with water (15 mL), and was washed with water, hexane, and hexane/ether (50:50). The product thus obtained (391 mg) contained 5% of starting aldehyde. It was dissolved in a mixture of ethanol (20 mL) and CH_2Cl_2. Rotor-evaporation of CH_2Cl_2 gave an ethanol suspension of the product (the latter is highly soluble in mixtures of these solvents while being considerably less soluble in neat solvents). The suspension was kept at −18 °C overnight. The product was filtered and washed with small amounts of ice-cold ethanol and hexane. After purification, it still contained 1% of aldehyde and was used as such. White solid: 305 mg (0.96 mmol, 70%). Anal. Calcd for $C_{13}H_7BrN_2O_3$ (MW 319.11): C, 48.93; H, 2.21; N, 8.78. Found: C, 48.52; H, 2.01; N, 8.55. ^{1}H NMR (400 MHz, DMSO-d$_6$): 8.56−8.49 (*py*, m, 1H), 8.28−8.20 (*py*, m, 2H), 8.16 (*bo*4, s, 1H), 7.91 (*bo*7, d, J 8.8, 1H), 7.69 (*bo*6, dd, J 8.4, J 0.8, 1H), CO_2H not observed. To drive the reaction to completion, one may stir and sonicate reaction mixture for a longer time.

Synthesis of Lanthanide Complexes. The reactions were performed under air using 3:3:1 molar ratio of the ligand, NaOH and $LnCl_3\ nH_2O$. The ligand was dissolved in hot THF (70−80 °C, 5 mL), followed by addition of NaOH dissolved in water (ca. 1 mL, used as a stock solution with ca. 100 mg of NaOH per 10 mL of water) and stirring for 5 min. In the case of HLBr it was necessary to add more water (1.5 mL) to dissolve its sodium salt which otherwise precipitated. A solution of $LnCl_3 \cdot nH_2O$ (n = 6 or 7; 99.9%, Aldrich) in ethanol/water (0.5/1.5 mL) was added dropwise over 5 min. A white precipitate formed upon addition. The suspension was stirred for 10 min at 70−80 °C, cooled to 40−50 °C over 10 min, and filtered while warm. The product was washed with THF/water (1:1), ethanol/water (1:1) and ether in that order. The complexes were dried under vacuum at room temperature. All complexes are white solids that are soluble in DMSO, boiling ethanol, boiling acetonitrile and are insoluble in hexane, ether and water. The use of aqueous ethanol as solvent in these reactions is not recommended because of the low solubility of the ligands which may result in the contamination of the complexes with unreacted ligand. Further synthetic details and analytical data for Eu complexes are provided below, while data for La, Nd, Gd, Tb and Yb complexes are given in the Supporting Information.

[Eu(LS)$_3$(H$_2$O)$_2$]·2H$_2$O. The reaction was performed with HLS (50 mg, 0.195 mmol), NaOH (7.80 mg, 0.195 mmol), and $EuCl_3 \cdot 6H_2O$ (23.83 mg, 0.065 mmol). Yield: 54 mg (0.055 mmol, 84%). Anal. Calcd for $C_{39}H_{21}EuN_6O_6S_3 \cdot 4H_2O$ (MW 989.84): C, 47.32; H, 2.95; N, 8.49. Found: C, 47.38; H, 2.82; N, 7.94.

[Eu(L)$_3$(H$_2$O)$_2$]·H$_2$O. The reaction was performed with HL (50 mg, 0.208 mmol), NaOH (8.33 mg, 0.208 mmol), and $EuCl_3 \cdot 6H_2O$ (25.42 mg, 0.069 mmol). Yield: 56 mg (0.061 mmol, 88%). Anal. Calcd for $C_{39}H_{21}EuN_6O_9 \cdot 3H_2O$ (MW 923.63): C, 50.71; H, 2.95; N, 9.10. Found: C, 51.16; H, 3.45; N, 8.66.

[Eu(LMe)$_3$(H$_2$O)$_2$]·H$_2$O. The reaction was performed with HLMe (50 mg, 0.197 mmol), NaOH (7.87 mg, 0.197 mmol), and $EuCl_3 \cdot 6H_2O$ (24.02 mg, 0.0656 mmol). Yield: 42 mg (0.043 mmol, 66%). Anal. Calcd for $C_{42}H_{27}EuN_6O_9 \cdot 3H_2O$ (MW 965.71): C, 52.24; H, 3.44; N, 8.70. Found: C, 52.44; H, 3.45; N, 8.13.

[Eu(LBr)$_3$(H$_2$O)$_2$]·THF. The reaction was performed with HLBr (50 mg, 0.157 mmol), NaOH (6.27 mg, 0.157 mmol) and $EuCl_3 \cdot 6H_2O$ (19.14 mg, 0.052 mmol). Yield: 48 mg

(0.040 mmol, 76%). Anal. Calcd for $C_{39}H_{18}Br_3EuN_6O_9 \cdot 2H_2O \cdot C_4H_8O$ (MW 1214.41): C, 42.53; H, 2.49; N, 6.92. Found: C, 43.04; H, 2.28; N, 7.38.

Acknowledgment. This research is supported by a grant from the Swiss National Science Foundation (No. 200020_119866/1).

Supporting Information Available: Synthesis of precursors, tetraethylammonium salts, and La, Nd, Gd, Tb and Yb complexes; ^{1}H NMR spectra of precursors, ligands, salts, and lanthanum complexes; absorption spectra of ligands and complexes; luminescence and excitation spectra of the complexes; CIF files of the crystal structures, CCDC 723978−723989. This material is available free of charge via the Internet at http://pubs.acs.org.